Unsupervised localization of heart and lung regions in EIT images: a validation study

Damien Ferrario[1], Andy Adler[1,2], Josesp Solà[1], Stephan Böhm[1] and Marc Bodenstein[3]

[1]CSEM - Centre Suisse d'Electronique et de Microtechnique, Switzerland
[2]Systems and Computer Engineering, Carleton University, Ottawa, Canada
[3]Department of Anesthesiology, Johannes Gutenberg-University Mainz, Germany

Abstract: We describe an algorithm for automatic detection of heart and lung regions in a time series of EIT images. Candidate regions are identified in the frequency domain and image based classification techniques applied. The algorithm was validated on a set of simultaneously recorded EIT and CT data in pigs. In 20 of 21 cases, identified regions in EIT images corresponded to those manually segmented in the matched CT image. Results confirm the accuracy of anatomical features in EIT images, as long as morphologically accurate information is used in EIT reconstruction.

1. Introduction

Electrical Impedance Tomography (EIT) generates images of the conductivity distribution in the body, using electrical stimulation and measurement at surface electrodes. EIT shows promise for monitoring blood and air movement in the thorax, driven by its ability to generate an image of the regional distribution of these phenomena. In order to evaluate a sequence of EIT images, it is important to accurately identify the relevant anatomical regions: the heart and lungs (H&L). Several methods have been used to identify lungs ROI within a sequence of EIT images. Hahn *et al* (1995) used the standard deviation and Kühnel *et al* (1997) the maximum linear regression, to compute images of the ventilation distribution. Pulletz *et al*. (2006) showed that both methods give similar results. One limitation to such work is the lack of validation against gold standards.

In this paper, we propose an improved procedure to detect H&L ROIs from EIT images, and then validate our method by comparing EIT-based ROIs to manually segmented CT regions.

2. Methods

Overview: This work was performed in four stages: 2.1) the EIT image sequence was reconstructed, 2.2) the image sequence was analysed with a novel algorithm which uses temporal and spatial information to detect and localize H&L regions, 2.3) the acquisition of simultaneous EIT and CT images, and 2.4) validation of detected regions against manually segmented CT images.

2.1. EIT morphological reconstruction

We reconstruct EIT images that correspond morphologically to the matched CT image. Normalized time difference EIT images of conductivity change are reconstructed from EIT measurements using a one-step Gauss Newton algorithm based on a finite element model (FEM) of the thorax shape. FEM models were generated using Netgen based on boundary shape and electrode positions take from the CT image of the specific subject. Such anatomically accurate models are an important factor in the precision of the results; this requirement is elaborated in the discussion section. The EIT sensitivity (Jacobian) matrix was calculated from a 3D tetrahedral

FEM of 20799 vertices, in which the identified 2D body boundary in the CT slice containing the electrode positions was extruded into the vertical direction by half the body width above and below the electrode plane. Images were reconstructed onto a coarser 2D FEM model (946 vertices), also constructed from the anatomical body shape, but without electrode refinement. Parameters in this model are chosen as follows: the prior estimate of covariance between image elements is set to be the Gaussian high pass filter; noise variance is modelled to be equal on all EIT data channels; and the Tikhonov factor was chosen heuristically to give a good compromise between noise and image resolution.

2.2. Unsupervised detection of the heart and lungs activity on EIT images

The goal is to automatically identify ROIs for the H&L from a sequence of EIT images ($x(i,t)$, with pixel index, i, and time index, t). Initially, cardiac and respiratory frequencies are estimated, and the energy of each pixel at both frequencies is calculated. Cardio-respiratory images are then generated by associating to each pixel an energy value. Finally, adjacent pixels with significant activity are identified and associated to the H&L ROIs (see fig. 1).
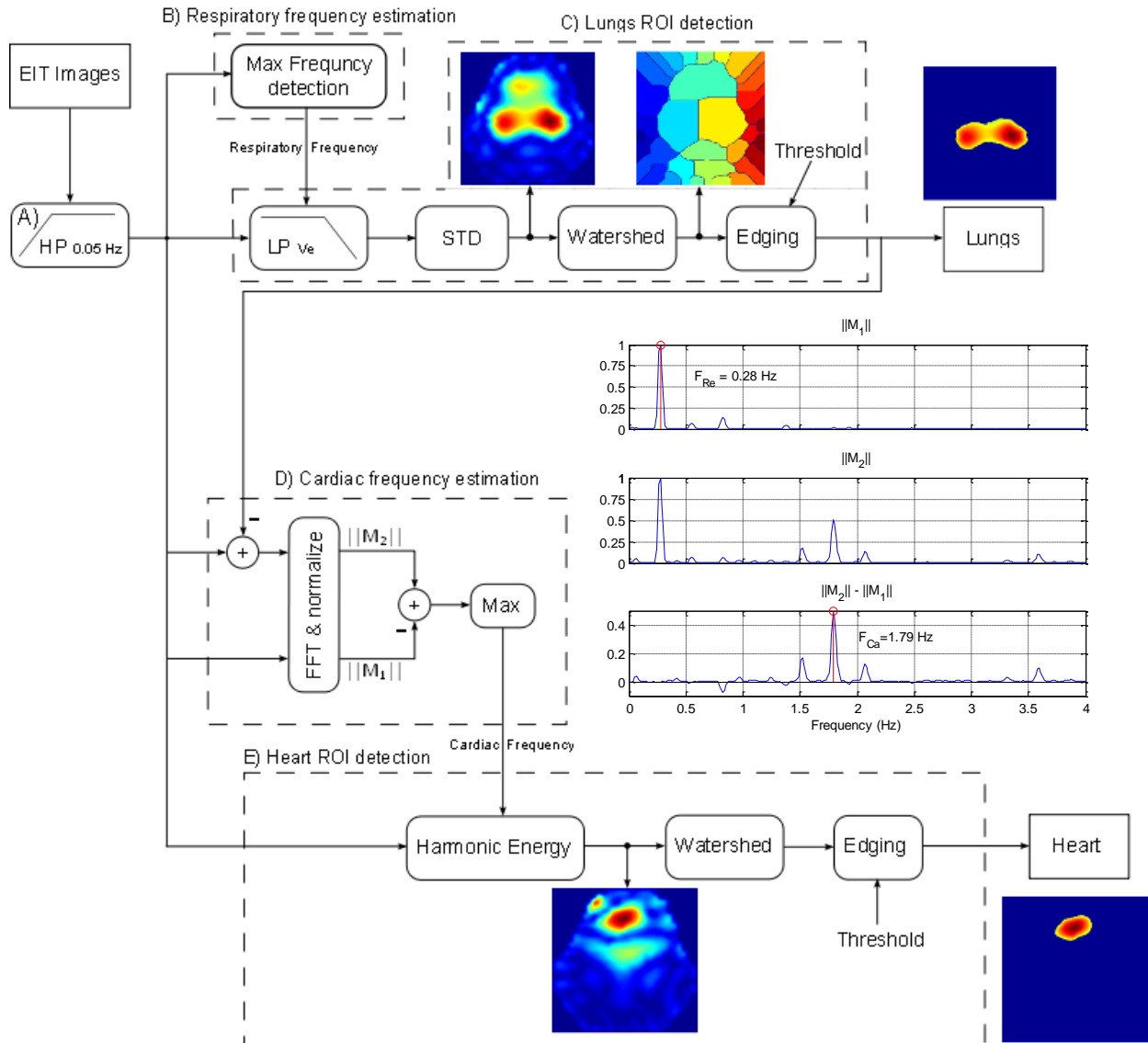
Fig. 1: Block diagram of the automatic detection of the lungs and heart activity using EIT.

Step A: a High Pass (HP) filter (cutoff frequency: 0.05 Hz, 4th order FIR filter) is applied to $x(i,t)$ to remove activity at low frequencies that is not related to heart or lungs activity.

Step B: the respiratory frequency f_{Re} is estimated. Initially, an averaged signal $m_1(t)$ is calculated. Respiratory frequency (f_{Re}), is then estimated as (example in fig. 1B):

$$M_1(f) = FFT(m_1(t)), \tag{1}$$

$$f_{Re} = \arg\max_f \|M_1(f)\|. \tag{2}$$

Step C: pixels depicting respiratory activity are detected and grouped together in a lung ROI, as suggested by Hahn *et al* 1995. $x(i,t)$ is Low Pass (LP) filtered (to get $x_{Re}(i,t)$) and the respiratory activity of each pixel is then estimated using a temporal standard deviation (std). Lungs ROI are identified via a watershed technique (Fernand 1994). The lungs ROI is assigned to the regions containing the two highest local maxima. Finally, a threshold, T is applied to respiratory activity levels, determining the ROI size.

Step D: the cardiac frequency (f_{Ca}) is estimated. The spectral content of all pixels not part of the lungs are summed ($m_2(t)$, with FFT $M_2(f)$); some respiratory component is still present but less than the image average. M_1 and M_2 are normalized and subtracted to highlight the cardiac frequencies. Cardiac frequency is estimated as:

$$f_{Ca} = \arg\max_f \|M_1(f)\| - \|M_2(f)\| \tag{3}$$

Heart activity of each pixel is then calculated by estimating the actual energy at the cardiac frequency of pixel time series via a non-parametric periodogram approach. Finally heart ROI is detected similarly to that of ventilation detection.

2.3. EIT and CT data acquisition methods.

To evaluate the accuracy of the measures calculated in 2.2, we compare the H&L regions identified in the EIT image to those in simultaneously acquired CT images. Data were acquired on healthy piglets (weighing 23±2 kg) according to a protocol approved by the responsible animal use committee for the University of Mainz, Germany (licence no. 1.5 177-07/401-75, Landesuntersuchungsamt Rheinland-Pfalz, 56028 Koblenz, Germany). Briefly, the protocol was as follows: The animals were investigated using static thoracic computed tomography at a CPAP level of 5, 15 and 45 mbar in apnea during the 25 seconds duration of the static CT (1 mm slices, HRCT: Somatotom Plus 4, Siemens, Erlangen, Germany). Simultaneously, EIT measurements were taken (using Goe-MF II EIT device, CareFusion, San Diego, CA, USA) with a sample frequency of 13 Hz controlled by MCFEIT study software (University of Goettingen, Germany).

For each animal, the CT slice corresponding to the electrode positions was taken and manually segmented by an expert to identify H&L regions. Inclusion criteria for analysis were: 1) healthy subject, with no obvious pneumonia or lung collapse, and 2) EIT electrode level at a position caudal to the maximum heart area in the CT.

2.4. Assessment of unsupervised algorithm accuracy

Detection accuracy was determined from measures of precision (P) as a function of the algorithm threshold, T, where P is the fraction of each EIT region within the corresponding regions in the CT image. Clearly, for very low T, all regions are identified, and P is low. We consider detection to be *accurate* if P becomes 100% at high T.

3. Results

An example algorithm output is shown in fig. 2. for different values of threshold. Note that identified ROIs are reasonable at all T values, but for high T values, only very central region

pixels are identified, *i.e.* maximizing the algorithm precision. In total, data from seven animals at three different PEEP levels were analysed, resulting in 21 tests, of which 20/21 were *accurate* for heart ROI detection and 21/21 for lungs. The single unsuccessful subject showed two separate heart ROIs, possibly due to movement of the heart during the cardiac cycle.
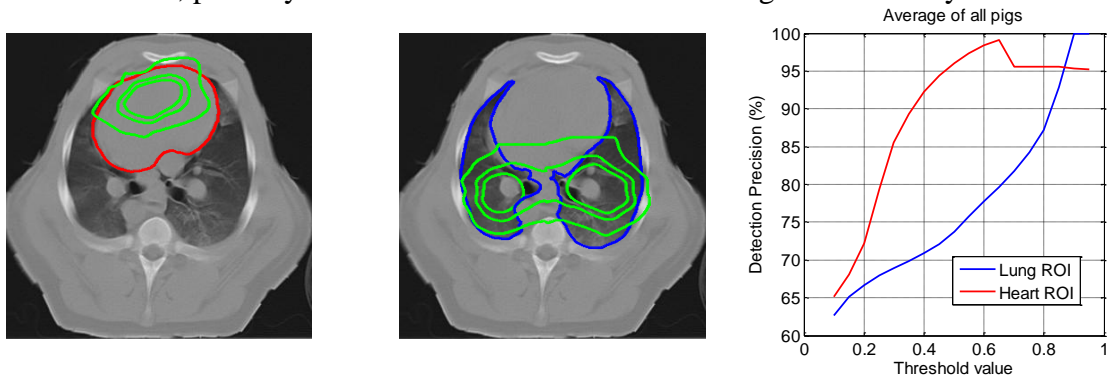
Fig. 2: Automatically identified heart and lung regions from EIT (green) with three level of T (0.25, 0.6 and 0.75) and the corresponding CT image (red and blue) at a PEEP of 5 mbar. Overall P vs threshold is shown for heart and lung regions (right).

4. Discussion

In this paper, we describe and evaluate an automatic algorithm to detect heart and lung regions in EIT images. Results show an accurate detection in almost all cases. Such results help validate EIT images as an accurate representation of physiological activity in the thorax, and provide additional support for physiological monitoring strategies based on EIT. Specifically, given accurate identification of anatomical regions in EIT images, it would be possible to specifically monitor organs or regions of interest.

Another significant finding in this project is the importance of accurate anatomical models for EIT reconstruction. While it is common to use average, or even circular models, to represent the thorax, we were able to use CT data to determine accurate thorax morphology and electrode locations. This results in much more anatomically-accurate EIT images (Fig. 3).
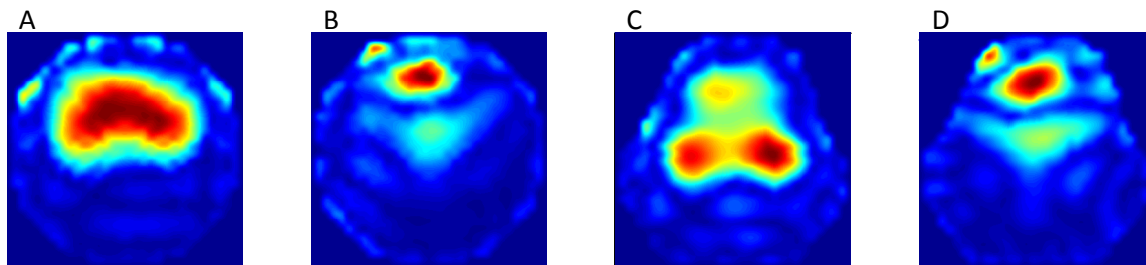
Fig. 3: Influence of morphologically accurate EIT reconstruction. Energy distribution at respiratory (A, C) and cardiac frequency (B, D). Accurate morphology images (A, B) show better correspondence to the lung anatomy and better separation of regions, compared to use of a circular model (C, D).

5. References

Fernand M, *Signal Processing* **38** 113–125, 1994
Hahn G, *et al*, *Physiol. Meas* **16** A161–73
Kerrouche N, McLeod CN, Lionheart WRB, *Physiol. Meas.* **22** 147, 2001
Kühnel G, *et al*, *Biomed. Technol. Berl.* **42** 213–4, 1997
Pikkemaat R, Leonhardt S, *J. Phys.: Conf. Ser.* **224** 012028, 2010
Pulletz S, Huibert R, *et al*, *Physiol. Meas* **27** S115-S127, 2006